AD_____

ENVIRONMENTAL FATE STUDIES OF HMX

(12)

Phase II - Detailed Studies

Final Report

by

Ronald J. Spanggord
William R. Mabey
Tsong-Wen Chou
Shonh Lee
Philip L. Alferness
Doris S. Tse
Theodore Mill

September 1983

Supported by:

U.S. ARMY MEDICAL RESEARCH AND DEVELOPMENT COMMAND
Fort Detrick, Frederick, Maryland 21701

SRI Project No. LSU-4412

Contract No. DAMD17-82-C-2100

SRI International
333 Ravenswood Avenue
Menlo Park, California 94025

Katheryn F. Kenyon, Contracting Officer Technical Representative
U.S. Army Medical Bioengineering Research and Development Laboratory
Fort Detrick, Frederick, Maryland 21701

SECURITY CLASSIFICATION OF THIS PAGE (When Data Entered)

REPORT DOCUMENTATION PAGE

READ INSTRUCTIONS BEFORE COMPLETING FORM

1. REPORT NUMBER

2. GOVT ACCESSION NO.

3. RECIPIENT'S CATALOG NUMBER

4. TITLE (and Subtitle)

Environmental Fate Studies of HMX

5. TYPE OF REPORT & PERIOD COVERED

Final Report, Phase II
February, 1983-September, 1983

6. PERFORMING ORG. REPORT NUMBER

SRI Project No. LSU-4412

7. AUTHOR(s)

Ronald J. Spanggord, William R. Mabey, Tsong-Wen Chou, Shonh Lee, Philip L. Alferness, Doris S. Tse, Theodore Mill

8. CONTRACT OR GRANT NUMBER(s)

DAMD17-82-C-2100

9. PERFORMING ORGANIZATION NAME AND ADDRESS

SRI International
333 Ravenswood Avenue
Menlo Park, California 94025

10. PROGRAM ELEMENT, PROJECT, TASK AREA & WORK UNIT NUMBERS

62720A.3E162720A835.AA.023

11. CONTROLLING OFFICE NAME AND ADDRESS

Commander
US Army Medical Research and Development Command
Fort Detrick, Frederick, Maryland 21701

12. REPORT DATE

September 1983

13. NO. OF PAGES

61

15. SECURITY CLASS. (of this report)

Unclassified

14. MONITORING AGENCY NAME & ADDRESS (if diff. from Controlling Office)

US Army Medical Bioengineering Research and Development Laboratory
Fort Detrick, Frederick, Maryland 21701

15a. DECLASSIFICATION/DOWNGRADING SCHEDULE

16. DISTRIBUTION STATEMENT (of this report)

Approved for Public Release; distribution unlimited

17. DISTRIBUTION STATEMENT (of the abstract entered in Block 20, if different from report)

18. SUPPLEMENTARY NOTES

19. KEY WORDS (Continue on reverse side if necessary and identify by block number)

HMX, Photolysis, Biotransformation, RDX, Environmental Assessment

20. ABSTRACT (Continue on reverse side if necessary and identify by block number)

This report describes studies that were performed to determine the impact of photolysis and biotransformation on the persistence of HMX in Holston River water and LAAP lagoons. In these environments, photolysis was found to be the dominant transformation process with half-lives ranging from 17 days in Holston River water to 7900 days in lagoon water. In the latter case, poor light transmission

DD FORM 1 JAN 73 1473

EDITION OF 1 NOV 65 IS OBSOLETE

SECURITY CLASSIFICATION OF THIS PAGE (When Data Entered)

19. KEY WORDS (Continued)

20 ABSTRACT (Continued)

through the lagoon water inhibited photolytic processes. Major photolytic transformation products were nitrate, nitrite, and formaldehyde.

Biotransformation of HMX occurred under both aerobic and anaerobic conditions in HMX wasteline water but conditions were not favorable for this transformation in Holston River water or in LAAP lagoon water. Therefore, biotransformation was not expected to contribute significantly to the loss of HMX in the environment. Under specialized conditions the biotransformation second-order rate constant was calculated to be 2×10^{-9} ml cell^{-1} hr^{-1} under aerobic conditions and 1.4×10^{-2} ml cell^{-1} hr^{-1} under anaerobic conditions. The metabolites resulting from both aerobic and anaerobic transformation were the mono- through tetra-nitroso derivatives of HMX which eventually were metabolized to 1,1-dimethylhydrazine.

Computer simulations of the Holston River and LAAP lagoons indicate that HMX will be persistent in these environments with dilution serving as the major factor in reducing HMX concentration in these water bodies.

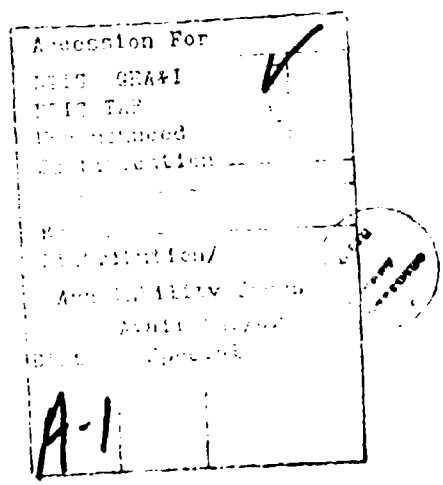

EXECUTIVE SUMMARY

This report describes studies that were performed to determine the impact of photolysis and biotransformation on the persistence of HMX in Holston River water and LAAP lagoons. In these environments, photolysis was found to be the dominant transformation process with half-lives ranging from 17 days in Holston River water to 7900 days in lagoon water. In the latter case, poor light transmission through the lagoon water inhibited photolytic processes. Major photolytic transformation products were nitrate, nitrite, and formaldehyde.

Biotransformation of HMX occurred under both aerobic and anaerobic conditions in HMX wasteline water but conditions were not favorable for this transformation in Holston River water or in LAAP lagoon water. Therefore, biotransformation was not expected to contribute significantly to the loss of HMX in the environment. Under specialized conditions the biotransformation second-order rate constant was calculated to be 2×10^{-9} ml $cell^{-1}$ hr^{-1} under aerobic conditions and 1.4×10^{-8} ml $cell^{-1}$ hr^{-1} under anaerobic conditions. The metabolites resulting from both aerobic and anaerobic transformation were the mono- through tetra-nitroso derivatives of HMX which eventually were metabolized to 1,1-dimethylhydrazine.

Computer simulations of the Holston River and LAAP lagoons indicate that HMX will be persistent in these environments with dilution serving as the major factor in reducing HMX concentrations in these water bodies.

FOREWORD

Citations of commercial organizations or trade names in this report do not constitute an official Department of the Army endorsement or approval of the products or services of these organizations.

TABLE OF CONTENTS

LIST OF FIGURES

LIST OF TABLES

I. INTRODUCTION

The production and manufacture of octahydro-1,3,5,7-tetranitro-1,3,5,7-tetrazocine (HMX) and HMX-containing explosives have led to the generation of wastewaters that are eventually discharged into aquatic environments. In order to assess the risk to mammalian and aquatic populations that may come in contact with such waters, it is important to know the mechanisms by which HMX is lost from wastewaters and the rate at which the loss occurs.

In Phase I of this study (Spanggord et al., 1982), we performed screening studies to identify the dominant transport and transformation processes that affect the persistence of HMX in the aquatic environment. We concluded that the loss of HMX would be governed by photolysis and, to a lesser extent, by biotransformation. This report describes detailed studies that were performed to estimate the rate constants for these processes.

Once the rate constants are known for dominant transport and transformation processes, it is possible to simulate specific environments through computer modeling. In this report, we simulated the Holston River near the Holston Army Ammunition Plant (HAAP) in Kingsport, Tennessee, and the waste disposal lagoons at the Louisiana Army Ammunition Plant (LAAP) in Minden, Louisiana. The results of these simulations can be used to project the HMX concentration as a function of time in these water bodies.

II. BACKGROUND

The approach to simulating selected environments is based on the assumption that the rate of loss of chemical (R) can be described as a simple second-order rate expression (Equation 1),

$$R = k[C][E] \quad , \tag{1}$$

where C is the concentration of chemical, E is an environmental parameter (such as light intensity, microbial population), and k is a second-order rate constant. Under conditions where E is constant, Equation 1 reduces to a pseudo-first-order rate expression,

$$R = k'[C] \quad . \tag{2}$$

Thus, the total loss of chemical can be described as the sum of all pseudo-first-order rate expressions, or

$$R_T = \sum_{i=1}^{n} k_i'[C] \quad . \tag{3}$$

For HMX, the total loss with respect to time is projected to be represented by Equation 4,

$$\frac{dC}{dt} = k_p[C] + k_b'[C] \quad , \tag{4}$$

where k_p and k_b' are the pseudo-first-order rate constants for photolysis and biotransformation, respectively. A brief discussion of the mathematical development of photolysis and biotransformation rate constants is given below.

A. Photochemical Transformation Rate

Chemicals undergo photochemical transformation in the aquatic environment through the absorption of photons at wavelengths of 290 nm and above. These wavelengths represent the solar spectrum penetrating the earth's upper atmosphere and reaching the surface.

The rate of absorption of light (I_A), by a chemical (C), at a particular wavelength in dilute solution in pure water can be determined by the following equation (Zepp and Cline, 1977):

$$I_A = 2.3r\varepsilon I_\lambda[C] = k_a[C] \quad , \tag{5}$$

where

ε = molar absorptivity in liters $cm^{-1}mole^{-1}$
I_λ = light intensity term in Einstein's $liter^{-1}s^{-1}$
[C] = chemical concentration in moles $liter^{-1}$
k_a = rate constant for light absorption
r = a correction term for water depth.

If the quantum yield, ϕ, represents the fraction of absorbed light leading to a chemical reaction, then the rate of chemical loss can be expressed as follows:

$$-\frac{dC}{dt} = I_A\phi = \phi k_a[C] = k_p[C] \quad , \tag{6}$$

where (at a single wavelength)

$$k_p = 2.3r\varepsilon\phi I_\lambda \quad . \tag{7}$$

Integration of Equation 6 gives

$$\ln \frac{C_o}{C_t} = k_p t \quad , \tag{8}$$

where C_o and C_t are concentrations of the chemical at time zero and at time t. This equation allows us to determine the rate constant for photolysis at a single wavelength from a regression fit of ln C_t, as a function of time, in which k_p is the slope of this first-order plot. Once k_p is known, the quantum yield, ϕ, is obtained from Equation 7, in which the molar absorptivity is measured from the absorption spectrum at the studied wavelength, and the light intensity is obtained by actinometry.

Because the quantum yield, ϕ, generally does not vary significantly with wavelength, the photolysis rate constant in sunlight, $k_p(s)$, can be represented as the quantum yield times the summation of the molar absorptivity times the light intensity over the solar spectral region:

$$k_p(s) = \phi \Sigma \varepsilon_\lambda I_\lambda \quad , \tag{9}$$

and the half-life in sunlight is

$$t_{1/2(s)} = \frac{\ln 2}{k_{p(s)}} \quad . \tag{10}$$

Values of ε_λ were obtained from laboratory measurements, whereas values for the sunlight intensity, I_λ, were obtained from the literature for a particular time of day, season, and latitude. The calculated rate constants, $k_{p(s)}$, were compared with the measured value, $k_{p(m)}$, obtained in pure water in sunlight using Equation 8. In our experience, the calculated and measured rate constants obtained by the above procedures are in close agreement, usually within a factor of two.

B. Biotransformation Rate

Many types of microorganisms are found in natural waters; the populations may vary with the type of water body, season, and organic

substrates being introduced. In this study, we attempted to obtain microorganisms biotransforming HMX by enrichment procedures using water from the HAAP HMX wasteline stream. These organisms can then be used to determine the biotransformation rate constant.

The biotransformation rate is a function of biomass and chemical concentration. When an organic chemical is utilized by microorganisms as the sole carbon source and its concentration limits the rate of microbial growth, the relationship between the chemical utilization rate and the chemical concentration can be expressed by the Monod kinetic equation as:

$$-\frac{dC}{dt} = \frac{\mu[X]}{Y} = \frac{\mu_m}{Y} \cdot \frac{[C][X]}{K_c + [C]} = k_b \frac{[C][X]}{K_c + [C]} \quad , \quad (11)$$

where [X] is the biomass per unit volume, μ is the specific growth rate, μ_m is the maximum specific grown rate, [C] is the concentration of growth-limiting chemical, K_c is the concentration of chemical supporting the half-maximum specific growth rate (0.5 μ_m), Y is the cell yield, and k_b is the substrate utilization constant and equal to μ_m/Y.

The parameters μ_m, Y, and K_c can be evaluated by performing a series of experiments with different chemical concentrations and low-level inocula or with continuous cultures (Smith et al., 1978). However, these methods are time-consuming, and large amounts of chemical are required.

For many pollutants in the environment, chemical concentrations are very low and $C << K_c$. Under these conditions, Equation 11 reduces to Equation 12, which is a simple second-order relation:

$$-\frac{dC}{dt} = k_b \frac{[C][X]}{K_c} = k_{b2}[C][X] \quad . \quad (12)$$

Furthermore, if the rate study is conducted using a large microbial population and a low chemical concentration, the bacterial cell count will remain constant under the experimental conditions because the cell growth will not be affected greatly by the consumption of the test chemical. The biotransformation rate is then assumed to be a pseudo-first-order rate process with respect to the chemical, C, and is described by Equation 13:

$$-\frac{dC}{dt} = k_b'[C] \quad , \tag{13}$$

where k_b' is a pseudo-first-order rate constant. Integration of Equation 13 yields Equation 14:

$$\ln \frac{C_o}{C_t} = k_b' t \quad , \tag{14}$$

where C_o and C_t are concentrations of chemical at time zero and at time t. By plotting ln C as a function of time, k_b' can be determined as the slope of the line.

Equation 12 shows that the rate of transformation is linearly related to the microbial population. Therefore, if the rate constant k_b' is measured with constant values of [X], the value of k_{b2} can be estimated from the relation (Equation 15):

$$k_{b2} = \frac{k_b'}{[X]} \quad , \tag{15}$$

where k_{b2} is the second-order rate constant and [X] is estimated from microbial plate counts.

C. Simulation Studies

Once the rate constants for the dominant transport and transformation processes are known for selected waters, computer models can be designed to simulate the loss and movement of the chemical in specific

water bodies. From these simulations, persistence of the chemical can be assessed and concentration/time-dependent curves can be constructed to project chemical concentrations as a function of time and distance from a discharge point. The modeling allows the effects of many variables to be investigated, such as chemical loading and hydrological parameters of the water body (flow rate, depth, etc). Seasonal variations can also be addressed by applying the proper rate constant (such as for photolysis) for specific times of the year, which allows one to estimate the periods of maximum and minimum transformation occurrance. Thus, through the model simulation, it becomes possible to estimate the environmental behavior of chemicals on both real-world and hypothetical bases.

III. METHODS AND RESULTS

A. Analytical Methods

1. HMX Analyses

A reverse-phase high-performance liquid chromatography (HPLC) system was used to quantify HMX and related compounds in water samples. In these analyses, a Water's radial compression module equipped with a Water's Radial-Pak C_{18} cartridge was used in conjunction with a water/acetonitrile or water/acetonitrile/methanol mobile phase system at a flow rate of 2.0 ml min^{-1}. Detection was by UV absorbance at 230 nm, and quantitation was performed by the internal standard method using 3,5-dinitrotoluene (3,5-DNT) or 1,3,5-trinitrobenzene (1,3,5-TNB) as the internal standard. The selection of parameters was based on the number of components present and the degree of resolution required.

Samples containing only HMX were analyzed isocratically using 45% acetonitrile in water as the solvent system and 3,5-DNT as the internal standard. When the water samples contained RDX (as did several of the HMX wastestream samples), the mobile phase consisted of (a) water and (b) methanol/acetonitrile (50/50). HMX and RDX were resolved using a linear gradient ranging from 30 to 60% (b) in (a) over 20 min and 3,5-DNT as the internal standard (Figure 1). Additional resolution was required when RDX metabolites appeared in biotransformation studies of HMX. This was accomplished with a linear gradient ranging from 10 to 70% (b) in (a) [with a 5-min hold at 10% (b)] in 30 min. In this case, the internal standard was 1,3,5-TNB (Figure 2).

The samples were prepared by adding 0.9 ml of the internal standard solution (in methanol) to 2.7 ml of sample. This ratio of sample

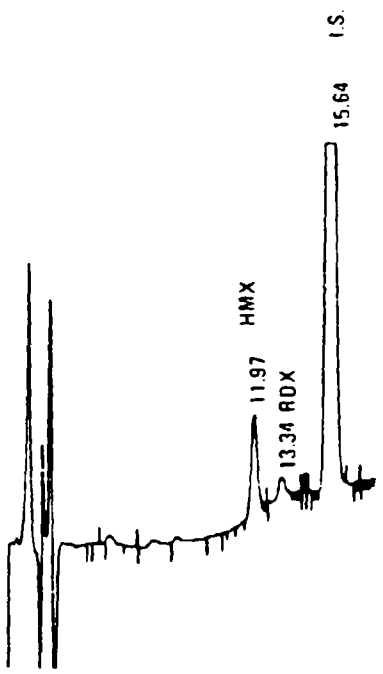

FIGURE 1 HPLC PROFILE OF HAAP HMX WASTE STREAM SAMPLES CONTAINING HMX AND RDX

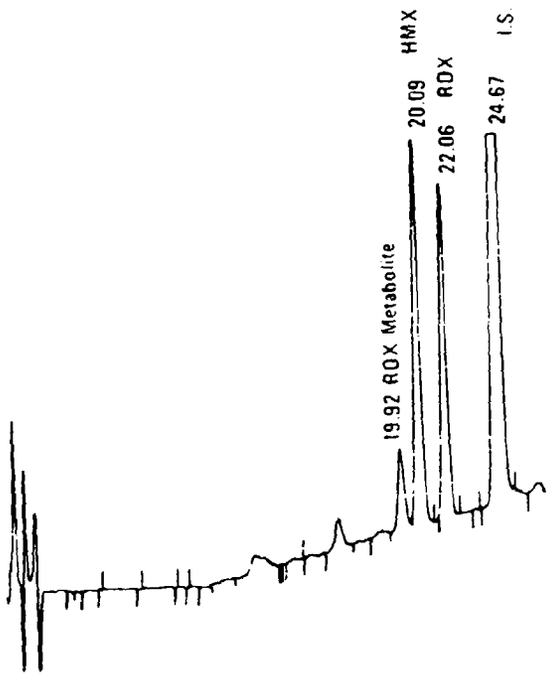

LA-4412-4

FIGURE 2 HPLC PROFILE OF RDX METABOLITES IN HMX BIOTRANSFORMATION STUDY

to internal standard served the dual purpose of minimizing sample dilution while approximating the solvent/water ratio of the mobile phase. The samples were then filtered through a 0.45-μm filter and injected into the liquid chromatograph. HMX was quantified using a relative response factor obtained from standard solutions that were periodicaliy analyzed in triplicate throughout the day of analyses. The results for four wastewater samplings are shown in Table 1.

TABLE 1

HPLC ANALYSIS OF HMX AND RDX IN HAAP HMX LINE WASTESTREAM

Date Sampled	HMX Found (ppm)	RDX Found (ppm)
5/24/82	0.59	0.33
9/18/82	1.00	---
2/28/83	2.65	6.92
6/6/83	0.90	0.33

2. Nitrite and Nitrate Analyses

The photochemical transformation of HMX gave nitrite and nitrate as two decomposition products. These compounds were analyzed by the direct aqueous injection of photolyzed solutions into a high-performance liquid chromatograph using a Whatman Partisil PXS 10/25 SAX anion exchange column and a 0.035 M phosphate buffer mobile phase system (pH 3.1) at a flow rate of 1.0 ml min^{-1}. Detection was by UV absorbance at 210 nm, and the anions were quantified by the external standard method.

3. Formaldehyde Analyses

A major photochemical transformation product was identified as formaldehyde by the Hantzsch reaction, in which formaldehyde is

coupled with 2,4-pentanedione to produce a highly fluorescent derivative when excited at 430 nm and observed at 520 nm.

A 2.0-ml aliquot of the sample was added to 2.0 ml of freshly prepared 0.05 M 2,4-pentanedione in 2 M ammonium acetate. The mixture was heated for 1 hr at 40°C and analyzed on a Baird SF-1 fluorometer equipped with a 430-nm excitation wavelength and fluorescence scanning from 400 to 600 nm. Formaldehyde was quantified from a calibration curve (peak height versus concentration) obtained from a series of standard formaldehyde solutions.

4. Organic Acids Analyses

Because of problems in sustaining HMX-transforming organisms from HMX wasteline waters, the waters were analyzed for small organic acids that might be critical to HMX biotransformation. HMX wasteline water samples (200 µl) were injected into an HPLC system containing an Interaction Chemicals ORH-801 organic acids column and a 0.002N H_2SO_4 aqueous mobile phase at a flow rate of 0.80 ml min^{-1}. Peaks were detected by UV absorbance at 210 nm, identified by elution volume, compared with known standards, and quantified by the external standard method. A chromatographic profile of HMX wasteline water samples, showing the presence of formic acid, acetic acid, propanoic acid, and other unidentified components, is presented in Figure 3.

5. Analytical Chemistry Discussion

HPLC methods with UV detection provide a direct means of monitoring HMX in aqueous environmental samples with a sensitivity of 0.1 ppm by direct aqueous injection. The availability of gradient elution programming on reverse-phase columns enhances the resolution of HMX, not only from its transformation products, but also from analog contaminants such as RDX, which appear along with HMX in wastewater and river water samples. This resolution also allows for the separation and collection of transformation products, which led to

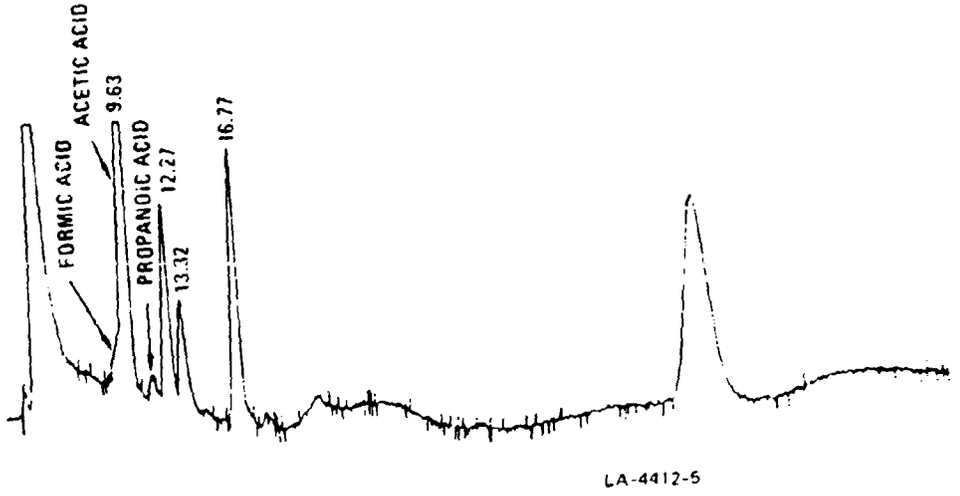

FIGURE 3 HPLC PROFILE OF ORGANIC ACIDS AND UNIDENTIFIED COMPONENTS IN HMX WASTE STREAM

their identification by probe-mass spectrometric techniques (see Section C, Biotransformation).

In the isolated wastestream samplings in this study, HMX concentrations ranged from 0.6 to 2.7 ppm, and RDX concentrations ranged from <0.1 to 7.0 ppm. Trace amounts of components with elution volumes corresponding to the mono-, di-, and tetranitroso-derivatives of HMX were also observed; however, the identification of these components could not be confirmed. Acetic acid was observed in the wastestream samples and in one case was quantified at 46 ppm. Formic and propionic acids were observed at lower levels, as were other unidentified carboxylic acid species. Thus, the wastestream profiles were not seen as overly complex when observed using UV detection at 254 and 210 nm, and the HPLC technique was determined to be ideally suited to follow HMX losses in various transformation processes.

B. Photochemical Studies

Photochemical studies were performed to measure the photochemical rate constant of HMX in pure water, in LAAP lagoon water, and in Holston River water. From these studies, the photochemical quantum yield was calculated according to Equation (7). Many of the above studies were conducted simultaneously with RDX, a structural analog of HMX, for comparative purposes. We carefully measured the UV absorbances of RDX and HMX above 299 nm and compared measured rate constants with those computed from the GC SOLAR program (R.G. Zepp, personal communication) using averaged seasonal light intensities for various latitudes. HMX photolysis products were investigated and a mechanism for the transformation of HMX in the solar spectral region was projected.

1. HMX and RDX Photolyses in Pure Water and in LAAP Water

Photolysis studies of HMX and RDX in pure water and in LAAP water were conducted between June 7 and June 17, 1983. LAAP water,

collected from LAAP Lagoon No. 9 in July 1982 and containing 5 ppm of HMX and 16 ppm of RDX, was used in these studies. Solutions of HMX and RDX in pure water were prepared at concentrations similar to those in LAAP water. The solutions were placed in two identical amber dishes cut from the bottoms of amber-colored gallon solvent bottles and filled to a depth of 4 cm. The two solutions were photolyzed side-by-side outdoors in weather that was mostly hazy in the mornings and sunny in the afternoons, with temperatures ranging from 19 to 32°C during the day. Two 4-ml aliquots were withdrawn each day after pure water had been added to adjust for water lost through evaporation. The aliquots were tightly capped, wrapped in aluminum foil, and refrigerated. On the last day of the experiment, all the samples were analyzed by HPLC. The results are plotted in Figure 4.

The photolysis rate constants for HMX and RDX in pure water (4.0 cm) were 0.19 and 0.56 day^{-1}, respectively, as calculated from Equation (8). The quantum yields calculated from the sunlight rate constants were 0.13 for HMX and 0.18 for RDX. These values are in good agreement with previous studies performed in April, in which quantum yields of 0.13 and 0.16 for HMX and RDX, respectively, were determined. The photolysis rate constants in LAAP water (4.0 cm deep) were 0.0099 day^{-1} for HMX and 0.057 day^{-1} for RDX. These data show that RDX is photolyzed approximately three times faster than HMX in pure water and six times faster than HMX in LAAP water, and imply that substances in LAAP water can promote the photolysis of RDX. The overall rate constants in LAAP water are smaller than those in pure water due to light screening. We found that 99% of the light is absorbed at a depth of 3.0 cm for all wavelengths shorter than 500 nm. These data are summarized in Table 2, and the observed rate constants are shown in Table 3.

Because HMX and RDX have similar structures, UV spectral absorbances, and photolysis quantum yields, we expected that they would be photolyzed at similar rates. To elucidate the difference in our observed rates, we photolyzed HMX and RDX in pure water in the

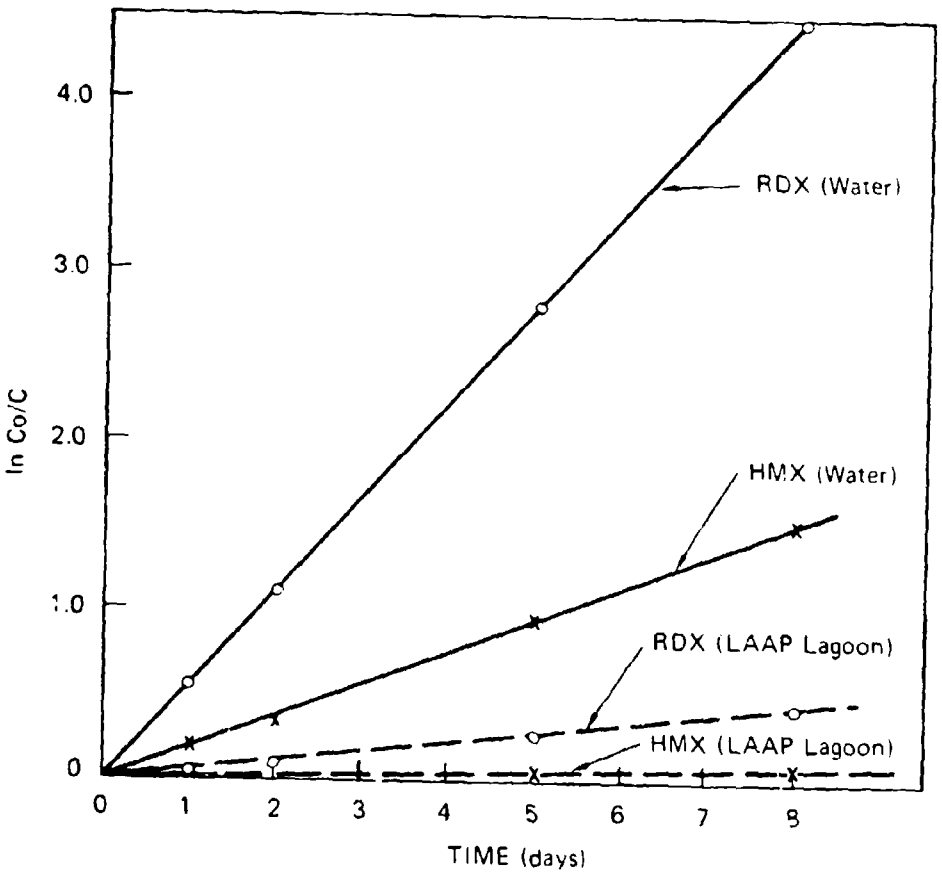

FIGURE 4 FIRST-ORDER SUNLIGHT PHOTOLYSIS PLOTS OF RDX AND HMX IN PURE WATER AND IN LAAP WATER

presence and absence of each other, in filtered LAAP water, and in LAAP water diluted with an equal volume of pure water. The photolyses were performed in borosilicate tubes in sunlight from June 30 to July 8, 1983. The results are shown in Table 4. In Experiment 1, we found that RDX is photolyzed nearly three times as fast as HMX. RDX photolysis also appears to be slightly sensitized by HMX or its photolysis products (Experiment 2), whereas HMX photolysis was not affected by the presence of RDX (Experiment 2). In LAAP water, diluted or not, HMX photolyzed at half the rate of RDX (Experiments 3 and 4).

Table 2

DEPTH WITH 99% ABSORBANCE AT DIFFERENT WAVELENGTHS AT 30°C

Wavelength, λnm	$\alpha_\lambda J\Delta$	Abs. (cm) Depth with 99%
290	0	0.51
340	7.41(19)	0.86
390	9.38(19)	1.09
440	1.33(20)	1.62
490	9.09(19)	3.17
505	7.00(19)	4.21

Table 3

OUTDOOR PHOTOLYSIS OF HMX AND RDX IN PURE WATER (PW) AND IN LAAP WATER

Solution	k_p d^{-1} for 4-cm dish		$k_p(RDX)/k_p(HMX)$
	HMX	RDX	
PW	0.19	0.57	2.9
LAAP	0.0099	0.057	5.7

Table 4

OUTDOOR PHOTOLYSIS OF HMX AND RDX IN PURE WATER (PW)
AND IN LAAP WATER IN BOROSILICATE TUBES
(June 30 to July 8, 1983)

Experiment	Solution	k_p d^{-1}	Rel. Rate to HMX in PW	ϕ
1	PW[1] HMX	0.302 ± 0.021	1.0	0.13
	PW[2] RDX	0.325 ± 0.016	2.7	0.18
2	PW[2] HMX	0.29 ± 0.012	0.96	--
	RDX	1.07 ± 0.08	3.5	--
3	0.5 LAAP HMX	0.14 ± 0.016	0.45	--
	RDX	0.34 ± 0.018	1.1	--
4	LAAP HMX	0.10 ± 0.005	0.34	--
	RDX	0.23 ± 0.008	0.76	--

PW[1] = Pure water containing only HMX or RDX.
PW[2] = Pure water containing both HMX and RDX.
0.5 LAAP = LAAP water diluted with equal volume of water.

To explain the differences in the photolysis rate constants of RDX and HMX, we reevaluated the molar absorptivity coefficient (ε_λ) of RDX and HMX at selected wavelengths, calculated the light absorption rate ($\varepsilon_\lambda L_\lambda$) at selected wavelengths, and determined the total rate of light absorption ($\Sigma\varepsilon_\lambda L_\lambda$) in the solar spectral regio.. These data are shown in Table 5 for the summer months. The total light absorption product for RDX was 4.58, whereas HMX had a total light absorption product of 2.29. The larger number for RDX results from larger molar absorptivity values from 314 nm to 400 nm compared with HMX. Thus, RDX is expected to be photolyzed at over twice the rate of HMX since ϕ for RDX is 20% larger.

Using published L_λ values and the computer program GC SOLAR (R.G. Zepp, personal communication), which is used to calculate day-averaged photolysis rate constants, we calculated the $\varepsilon_\lambda L_\lambda$ product from 290 to 410 nm and plotted this value versus wavelength for RDX and HMX (Table 6 and Figure 5). This program predicted a difference by a factor of 2 in the photolysis rates of RDX and HMX, again reflecting the significant differences in their molar absorptivity coefficients in the solar spectral region above 314 nm.

Table 5

ε_λ VALUES OF HMX AND RDX AND
$\varepsilon_\lambda L_\lambda$ VALUES AT 40°N

		ε_λ (M^{-1} cm^{-1})		$\varepsilon_\lambda L_\lambda$	
λ nm	L_λ (summer)	HMX	RDX	HMX	RDX
299	2.49(-4)	171	164	0.043	0.048
304	2.32(-3)	103	112	0.240	0.260
309	7.93(-3)	60	75	0.476	0.595
314	1.81(-2)	33	49	0.597	0.887
319	2.91(-2)	17	26	0.495	0.757
323	2.97(-2)	8.8	18.1	0.261	0.538
340	3.54(-1)	0.48	2.8	0.170	0.991
370	4.58(-1)	0.017	0.7	0.008	0.321
400	9.71(-1)	0	0.2	0	0.194
430	1.28	0	0	0	0
$\Sigma\varepsilon_\lambda L_\lambda$				2.29	4.58

2. HMX and RDX Photochemical Rate Constants for the Holston River

In Phase I, we calculated the photolysis rate constant for HMX in the Holston River in late spring to be 1.66×10^{-1} day^{-1}, with no

Table 6

Light Intensity of RDX and HMX at Each Wavelength at 40% as Calculated by GC SOLAR

Obs	λ, nm	I_λ (Sum 40)	σ_λ (RDX)	σ_λ (HMX)	$I_{\sigma\lambda}$ (RDX)	$I_{\sigma\lambda}$ (HMX)
1	2.975E+02	6.170E-05	1.980E+02	2.000E+02	1.222E-02	1.234E-02
2	3.000E+02	2.700E-04	1.500E+02	1.580E+02	4.050E-02	4.266E-02
3	3.025E+02	8.300E-04	1.240E+02	1.220E+02	1.029E-01	1.013E-01
4	3.050E+02	1.950E-03	1.040E+02	9.200E+01	2.028E-01	1.794E-01
5	3.075E+02	3.740E-03	8.600E+01	7.000E+01	3.216E-01	2.618E-01
6	3.100E+02	5.170E-03	7.000E+01	5.600E+01	4.319E-01	3.455E-01
7	3.125E+02	9.070E-03	5.600E+01	4.400E+01	5.079E-01	3.991E-01
8	3.150E+02	1.220E-02	4.400E+01	3.200E+01	5.368E-01	3.904E-01
9	3.175E+02	1.550E-02	3.300E+01	2.200E+01	5.115E-01	3.410E-01
10	3.200E+02	1.870E-02	2.470E+01	1.380E+01	4.619E-01	2.581E-01
11	3.231E+02	3.350E-02	1.810E+01	8.800E+00	6.064E-01	2.948E-01
12	3.300E+02	1.160E-01	8.400E+00	2.800E+00	9.744E-01	3.248E-01
13	3.400E+02	1.460E-01	2.800E+00	4.800E-01	4.088E-01	7.008E-02
14	3.500E+02	1.620E-01	1.200E+00	9.000E-02	1.944E-01	1.458E-02
15	3.600E+02	1.790E-01	8.000E-01	2.600E-02	1.432E-01	3.580E-03
16	3.700E+02	1.910E-01	7.000E-01	1.700E-02	1.337E-01	3.247E-03
17	3.800E+02	2.040E-01	6.000E-01	1.300E-02	1.224E-01	2.652E-03
18	3.900E+02	1.930E-01	4.000E-01	5.400E-03	7.720E-02	1.042E-03
19	4.000E+02	2.760E-01	2.000E-01	0.000E+00	5.520E-02	0.000E+00
20	4.100E+02	3.640E-01	0.000E+00	0.000E+00	0.000E+00	0.000E+00

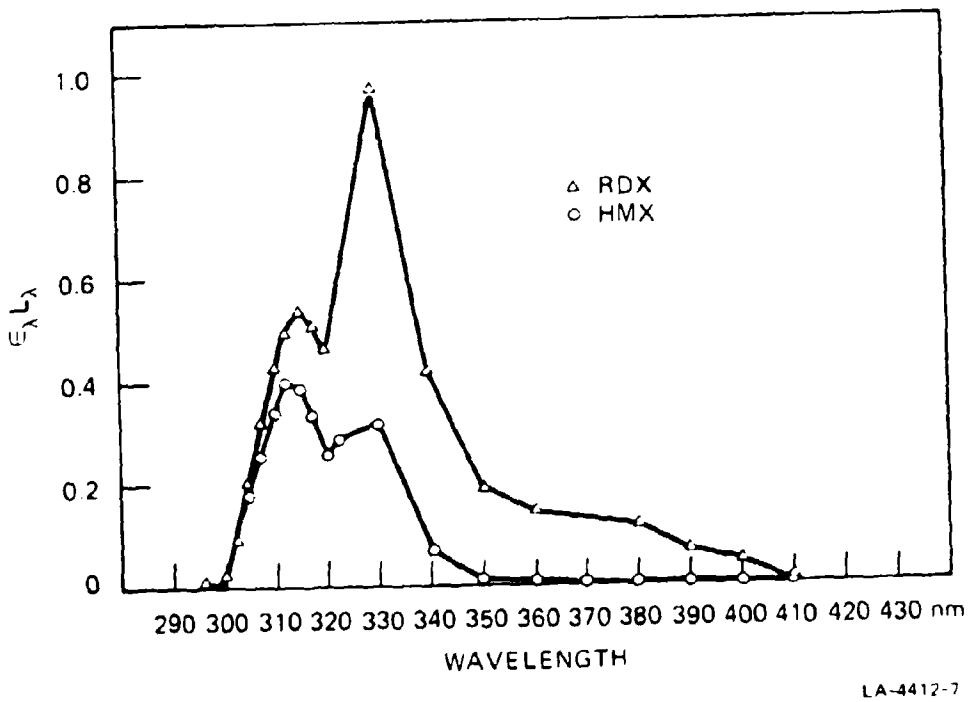

FIGURE 5 PLOT OF $\epsilon_\lambda L_\lambda$ VALUES VERSUS WAVELENGTH FOR HMX AND RDX FROM G.C. SOLAR

significant difference between rate constants of waters obtained above or below the Holston Army Ammunition Plant. Using the GC SOLAR program, we calculated the photolysis rate constants for HMX and RDX at depths ranging from 0 to 300 cm for the four seasons. These data are shown in Table 7. The calculated and measured rate constants again differed by a factor of 2 (1.66×10^{-1} d^{-1} versus 3.31×10^{-1} d^{-1} for late spring), which may reflect the difference between the actual and calculated light intensities on the day of the experiment. A factor of 2, however, is considered acceptable for modeling purposes.

For the modeling study, rate constants were interpolated for depths of 180 to 360 cm. These depths were derived from streambed contours of the Holston River obtained from a previous study (Spanggord et al., 1981).

Table 7

CALCULATED FIRST-ORDER PHOTOLYSIS RATE CONSTANTS FOR HMX AND RDX IN HOLSTON RIVER WATER AS A FUNCTION OF DEPTH FOR THE FOUR SEASONS

	k_p d^{-1}			
Depth (cm)	Spring	Summer	Fall	Winter
		HMX		
0	0.286	0.400	0.16	0.069
50	0.087	0.120	0.045	0.021
100	0.045	0.063	0.024	0.011
150	0.030	0.042	0.016	0.0073
200	0.023	0.032	0.012	0.0055
250	0.018	0.025	0.010	0.0044
300	0.015	0.021	0.0080	0.0036
		RDX		
0	0.71	0.94	0.40	0.20
50	0.25	0.32	0.13	0.070
100	0.14	0.18	0.073	0.039
150	0.092	0.12	0.049	0.026
200	0.069	0.089	0.037	0.020
250	0.055	0.072	0.030	0.016
300	0.046	0.060	0.025	0.013

3. HMX Photolysis Products and Photolysis Mechanism

In the sunlight experiments, we observed the formation of nitrite, nitrate, and formaldehyde as stable end transformation products, with no evidence for the formation of N-nitroso derivatives resulting from N-O bond cleavages from solar radiation. In each experiment, only 50% of the nitro groups could be accounted for as nitrite and nitrate ions per mole of HMX consumed. In following the rate of production of these species, nitrite was always generated first. However, it is difficult to provide a conclusive photochemical mechanism for HMX transformation, because nitrite and nitrate also undergo photolytic transformations (Zafirou, 1974). These secondary reactions may obscure the analysis of how the initial steps of the transformation occur.

Our findings correlate with several of the mechanistic steps proposed by Glover and Hoffsommer (1979) for the photolysis of RDX. An overall mechanistic scheme is presented in Figure 6. This scheme is based on our findings of an initial production of nitrite with nitrate concentrations increasing on extended photolysis. With only 50% of the HMX nitro group accounted for as nitrite and nitrate, the remaining nitro groups and ring nitrogens are converted to dinitrogen oxide, ammonia, and formamide, as proposed for the hydrolysis of methylenedinitroamine intermediates (Lamberton et al., 1979).

4. Photochemistry Discussion

The photolysis of HMX proceeds by a direct photolytic mechanism, with a HMX half-life of approximately 1.4 days in pure water and 1.7 days in Holston River water (4 cm deep) during the summer months. Light attenuation by UV-absorbing species (LAAP lagoon water) increased the half-life to 70 days under identical conditions of light intensity and depth. In either case, the loss rate appeared to be unaffected by cosubstrates (such as RDX) in solution.

Depth also plays an important role in estimating the photochemical half-life of HMX. At depths where >99% of the light is absorbed (3.0 cm in LAAP lagoon water; 20 cm in Holston River water), the photolysis half-life is directly proportional to depth. Thus, water body absorptivity and depth must be considered in predicting HMX photolysis half-lives in selected water bodies.

In these studies, we observed that RDX photolyzed nearly two to three times faster than HMX. Although the compounds have similar quantum yields, we determined that small differences in their molar absorptivity coefficients in the 320 to 400 nm range were sufficient to account for the observed differences in photolysis rates, even though RDX photolysis was sensitized, either by HMX or by HMX and RDX photolytic transformation products.

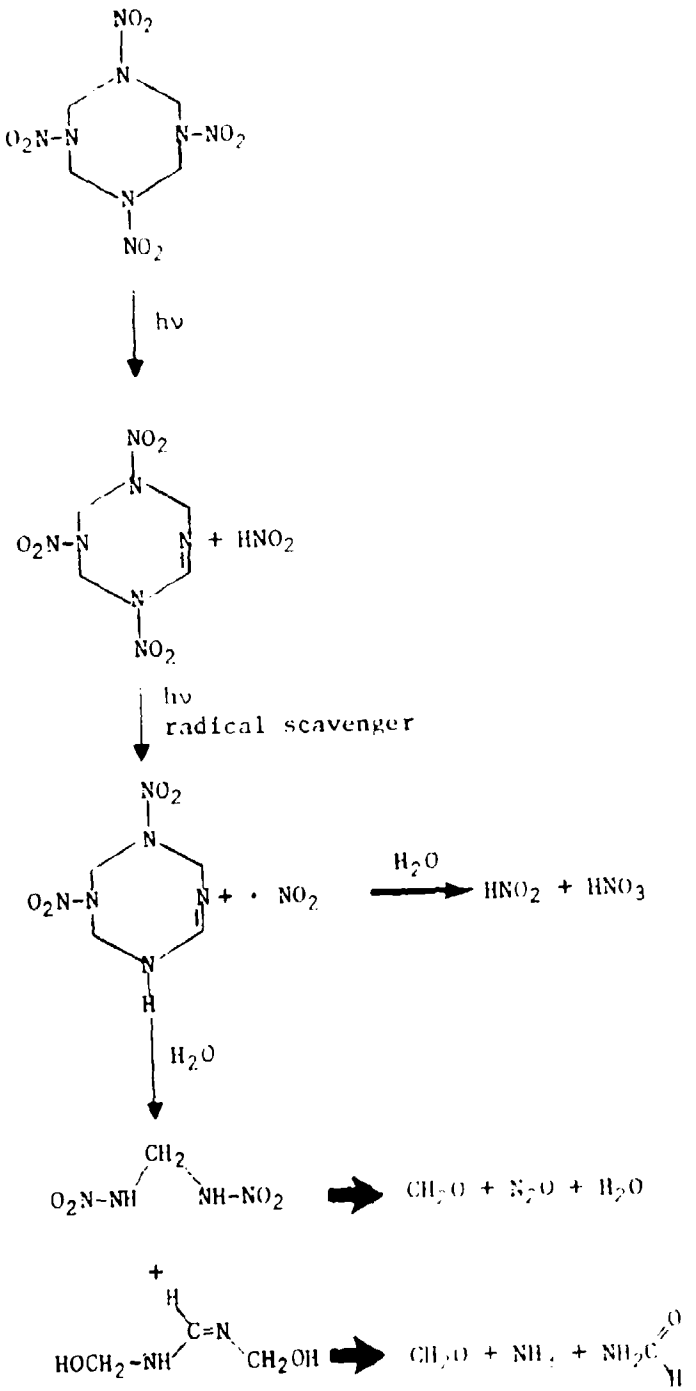

Figure 6. PROPOSED MECHANISM FOR THE SOLAR PHOTOLYSIS OF HMX IN WATER

Once light is absorbed by HMX, initiating the reaction, the molecule rapidly decomposes, as evidenced by no immediate buildup of intermediate products. This is consistent with what other workers have found in the photolysis of RDX (Glover and Hoffsommer, 1979). Thus, photolytic end products are believed to consist of nitrite, nitrate, formaldehyde, acetamide, ammonia, and dinitrogen oxide.

C. Biotransformation

1. Aerobic Biotransformation

In the screening studies, we observed that HMX was aerobically transformed when yeast extract was added to Holston River water. However, we were unable to produce an enriched culture by successive transfers of organisms to HMX-containing flasks. To determine whether HMX-transforming cultures could be obtained from local areas, we obtained water samples from Searsville Pond in Woodside, California, and from Coyote Creek in San Jose, California. To 2 liters of each water sample, we added 4 ppm of HMX with or without the addition of 50 ppm of yeast extract. Then the sample mixtures were incubated for 20 days. At the end of that time, HMX was not significantly transformed in any of the water samples.

To obtain the aerobic HMX-biotransforming organism again, water from the HMX effluent line at the Holston Army Ammunition Plant was shipped to SRI and received on February 28, 1983. Analysis of this water by HPLC showed that it contained 2.6 ppm of HMX and 7.0 ppm of RDX. HMX was added to the water to increase its concentration to 6.1 ppm, and 50 ppm of yeast extract was also added. After 2 days of incubation, RDX was transformed aerobically to 0.1 ppm, and HMX decreased to 3 ppm by HPLC analysis. When the organisms were inoculated into 100 ml of basal salts medium (BSM) along with 4 ppm of HMX and 50 ppm of yeast extract, no HMX transformation occurred, which was consistent with our previous findings (Spanggord et al., 1982).

On the assumption that some components in the wastewater may help the HMX biodegradation, the microorganisms in the degraded water sample and 50 ppm of yeast extract were also inoculated into the medium made of the refrigerated HMX wasteline water sample. HMX in the first transfer flask decreased from 4.8 ppm to 2.7 ppm after 5 days of incubation, and RDX decreased from 7.0 to 1.2 ppm. However, HMX biotransformation became less and less in successive transfers. HMX decreased from 4.0 to 3.2 ppm in the fourth transfer flask, and from 3.9 to 3.5 ppm in the sixth transfer flask. The addition of 60 ppm of Sabouraud dextrose broth (SDB) failed to substain the transformation, and an enriched culture was not obtained.

Microscopic examination of the wastewater revealed the presence of fungi as well as bacteria in the water. Suspecting that a fungus may be responsible for the HMX transformation, we streaked a water sample on Sabouraud's dextrose agar (SDA) and allowed the organisms to grow. The grown organisms were inoculated into BSM with 4 ppm of HMX and 60 ppm of SDA broth and were then incubated statically in an incubator. Although fungi grew well in the medium, no biotransformation was observed in these flasks.

A continuous-culture system was also set up for the acclimation of HMX-utilizing microorganisms. HMX wasteline water in a refrigerated water bath was continuously pumped into a 58-ml growth chamber at a dilution rate of 0.04 ml/min (retention time equivalent to one volume change per day). Initially, the solution contained 300 ppm of yeast extract, and 300 ppm of glucose was added with an infusion pump at a rate of 4.8 ml per day. Later, this solution was replaced by a solution containing 200 ppm of yeast extract and 800 ppm of SDA broth, which was added at a rate of 3.6 ml per day. The water medium in the growth chamber was aerated and mixed by gently bubbling air through it. We observed good growth of fungi and bacteria in the continuous culture. The effluent was then cascaded into four successive continuous-culture growth chambers. However, the analysis of HMX and RDX in the first and last chambers showed that no transformation of these

chemicals was occurring. Thus, it appears that factors critical to the aerobic transformation of HMX are still unknown.

Another experiment was performed with refrigerated wastewater (5 weeks). The water was enriched with 50 ppm yeast extract and 60 ppm of SDB, and 1 ppm of HMX was added to make the final HMX concentration 3.5 ppm. After 3 days, RDX was reduced from 5.0 ppm to a nondetectable level. The HMX concentration decreased to 2.8 ppm but did not decrease further. Again, transfer of these organisms into BSM/50 ppm yeast extract/60 ppm SDB/4 ppm HMX medium did not transform HMX, and the transfer of organisms to wasteline water/yeast extract/SDB medium (HMX made up to 50 ppm) showed that the organisms had gradually lost their ability to transform HMX.

Because the HMX wasteline water contained acetic acid, formic acid, and propionic acid, the effect of acetate on aerobic biotransformation was tested. To HMX wasteline water that had been refrigerated for 6 weeks, we added 100 ppm of sodium acetate or yeast extract and 1 ppm of additional HMX to make a final HMX concentration of 4.3 ppm. The HMX in acetate-supplemental water did not transform in 7 days, whereas the HMX in yeast extract-supplemental water decreased to 2.9 ppm at Day 3 and to 2.7 ppm at Day 7.

Wastewater from HAAP was collected again on May 24 and was received at SRI on May 31, 1983. This water contained 2.1 ppm of HMX. To this water was added 2 ppm of additional HMX and 20 ppm each of yeast extract, sodium acetate, sodium propionate, and sodium benzoate. After 3 days of incubation, HMX concentration decreased from 4.1 ppm to 0.22 ppm. The transformation had a first-order rate constant of 4×10^{-2} hr^{-1}. However, successive transfers of these organisms in the same composition of water medium did not result in an enriched culture.

Another wasteline water sample was collected on June 7 and was received on June 8, 1983. This sample contained 0.9 ppm HMX and 0.3 ppm RDX. However, this water did not support the biotransformation

of HMX when either yeast extract alone or a mixture of yeast extract, acetate, propionate, and benzoate was added.

Because enrichment organisms were not obtained, a detailed rate study could not be conducted. Therefore, we estimated the rate constant based on the biotransformation of HMX in incubation bottles from the May test sample and on previous tests conducted in Phase I studies. The first-order rate constant was measured to be $k_b' = 4 \times 10^{-2}$ hr^{-1}. The bacterial count of the water at Day 1 of incubation was 2×10^7 colony-forming units (CFU) ml^{-1}. Therefore, the second-order rate constant, k_{b2}, was calculated to be 2×10^{-9} ml $cell^{-1}$ hr^{-1}.

If the natural water sample contained 1×10^5 CFU/ml microorganisms, then the first-order rate constant would be 2×10^{-4} hr^{-1} (Equation 15). This corresponds to a half life of 3465 hr ($\ln 2/2 \times 10^{-4}$), or 144 days, under these specialized conditions.

2. Anaerobic Biotransformation

In the screening studies, we were able to grow anaerobic HMX-transforming organisms in transferring flasks containing 4 ppm of HMX, 50 ppm of yeast extract, and BSM. To study the effect of yeast extract concentration on HMX transformation, we added 10, 30, or 50 ppm of yeast extract to 3.5 ppm of HMX in BSM and inoculated the flasks with HMX-transforming organisms. The HMX concentration in these media after 3 days of anaerobic incubation was 2.8, 1.5, and <0.2 ppm, respectively, and the anaerobic bacterial counts were 4.2×10^5, 1.7×10^6, and 2.2×10^6 CFU ml^{-1}, respectively. Thus, we can project that the higher the concentration of yeast extract, the greater the population of bacteria that utilize HMX, resulting in a faster rate of transformation of HMX than that found with lower yeast concentrations.

Because acetic acid and other short-chain organic acids were found in wasteline water samples, acetic acid and other organic

compounds were tested as supplemental nutrients. To BSM/4 ppm HMX medium we added 50 ppm each of glucose, Difco protease peptone No. 3, sodium acetate, or yeast extract. The percent of HMX transformation is shown in Table 8.

Table 8

PERCENT OF HMX TRANSFORMED ANAEROBICALLY WITH SUPPLEMENTAL NUTRIENTS

Supplemental Nutrient	HMX Transformed (%) Day 1	Day 2
Glucose	30	75
Peptone	27	85
Na Acetate	24	77
Yeast Extract	35	76

All the nutrients tested apparently have similar effects on anaerobic HMX biotransformation.

Biotransformation was also studied using grown and washed cells. Organisms grown for 4 days in three 1-liter flasks containing 4 ppm HMX and 50 ppm BSM were centrifuged, washed, and resuspended in one-tenth volume of BSM. Centrifuge bottles were flushed with nitrogen gas during the handling. Four ppm of HMX were added to the cell suspension, and 20 ml of suspension were dispensed into 30-ml serum bottles with 50 ppm or 100 ppm of yeast extract, 50 ppm glucose, or 50 ppm Difco protease peptone No. 3. The bottles were flushed with nitrogen gas and capped with rubber stoppers. After 3 hr of incubation, HMX was transformed from 4.0 ppm to 1.1, 0.3, 2.1, and 2.6 ppm in the cell suspension with 50 ppm yeast extract, 100 ppm yeast extract, 50 ppm glucose, and 50 ppm peptone, respectively. The transformation slowed afterwards, presumably because the nutrient had been exhausted. These results show that yeast extract is better than glucose or peptone for HMX biotransformation by grown cells, and that

higher concentrations of yeast extract accelerate the transformation rate. HMX was not transformed in the cell suspension when no nutrient was added. With 50 ppm of yeast extract, a first-order rate constant was calculated to be 0.43 hr^{-1} with an anaerobic bacterial count of 3 $\times 10^7$ CFU ml^{-1}. A second-order rate constant (k_{b_2}) was calculated to be 1.4×10^{-8} ml $cell^{-1}$ hr^{-1}.

3. Metabolite Identifications

The HPLC profiles for the anaerobic biotransformation of HMX after 1, 2, and 3 days of incubation are shown in Figure 7. The profiles indicate the presence of five metabolites, which were collected from the HPLC by repetitive injection.

The collected fractions were analyzed by mass spectrometry using desorption electron impact, positive ion desorption chemical ionization, and negative ion desorption chemical ionization. The first eluting component was identified as octahydro-1,3,5-tetranitroso-1,3,5,7-tetrazocine, based on the positive ion spectrum yielding a molecular ion plus 18 at 250 amu (molecular weight 232) and on the negative ion spectrum showing the addition of mass fragments to the molecular ion, which was consistent with the behavior of RDX and HMX reference compounds (Figures 8 and 9) under the same conditions. The electron impact spectrum gave little information. The spectra for this metabolite are shown in Figure 10. The spectra of the remaining metabolites showed fragmentation behavior similar to that of the tetranitroso derivative (Figures 11 to 14) and were identified as the tri-, di-, and mono nitroso derivatives of HMX. The dinitroso derivative was present as two isomers (1,2- and 1,3-dinitroso derivatives) showing a nonselectivity of nitro group reduction. Thus, the anaerobic metabolism of HMX is initiated by the successive reduction of the nitro groups, as shown in Figure 15.

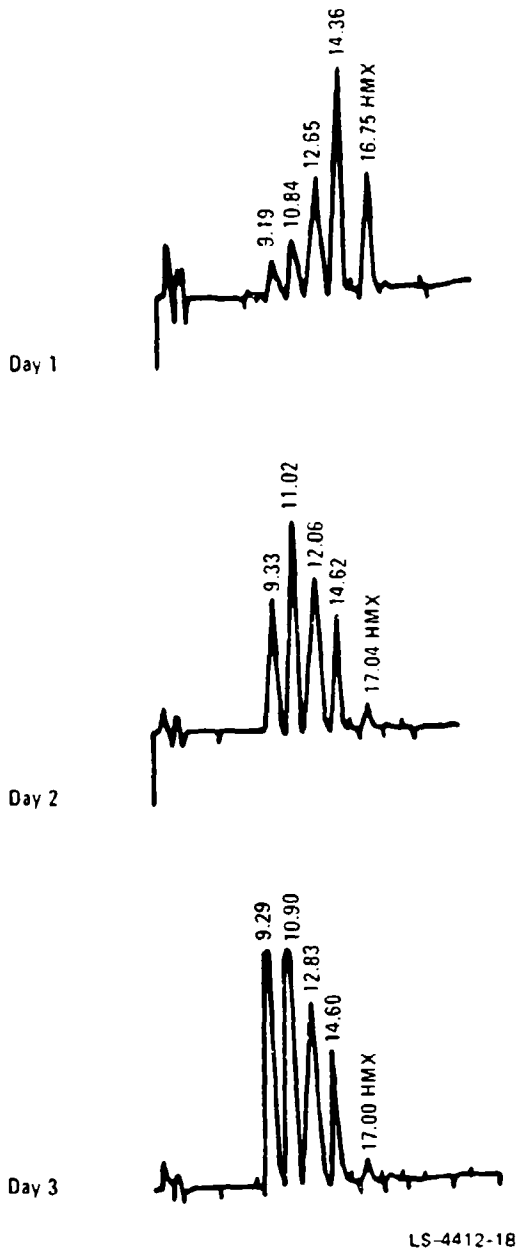

FIGURE 7 HPLC PROFILE OF HMX METABOLITES ON DAYS 1, 2, AND 3

Waters Radial Pak-A C_{18} cartridge; Solvent: 20-40% B in A, where A is water and B is methanol acetonitrile (50:50) in 20-min linear gradient; Flow: 2 ml/min; Detection: UV @ 230 nm

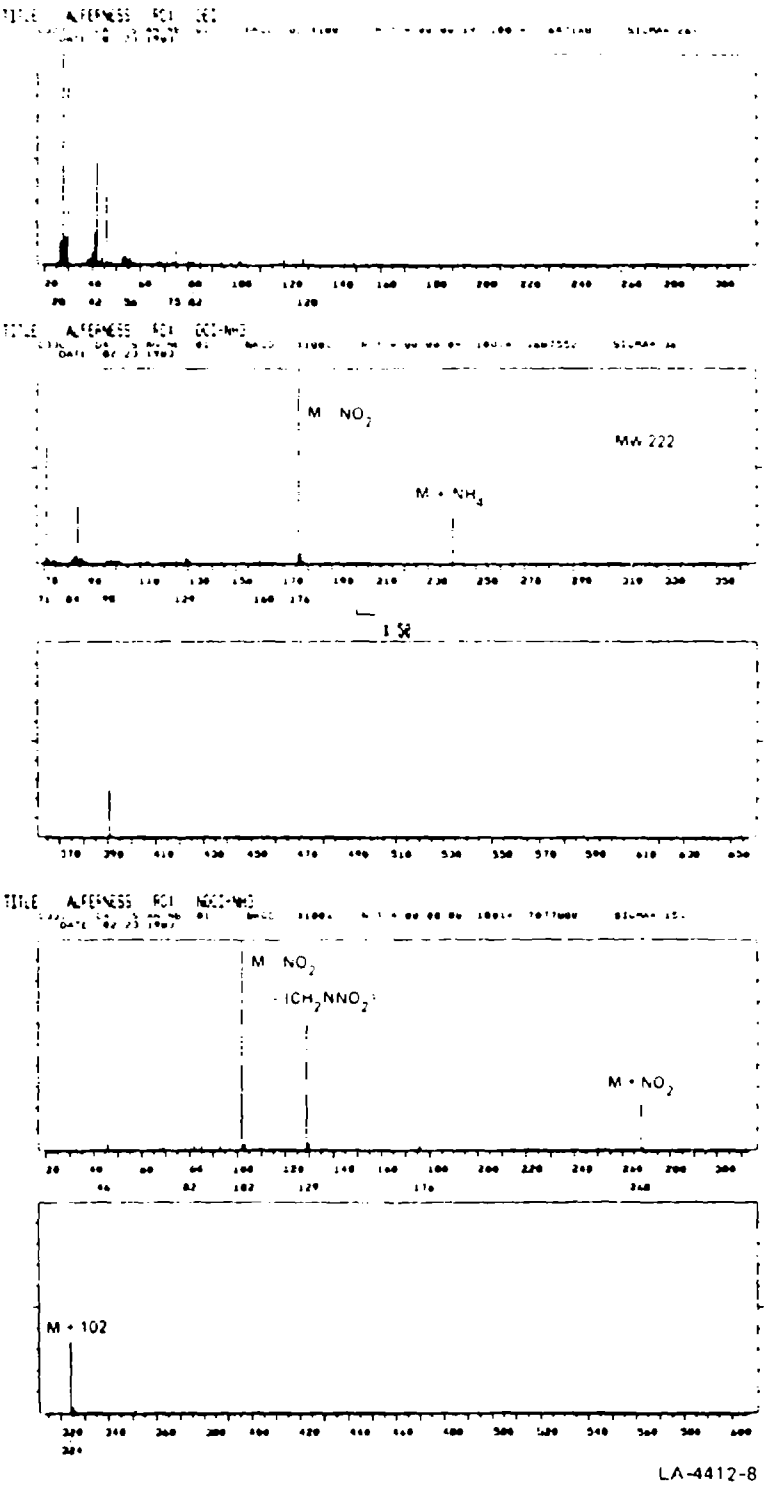

FIGURE 8 MASS SPECTRA FOR RDX

(a) Electron impact (b) Positive ion (c) Negative ion

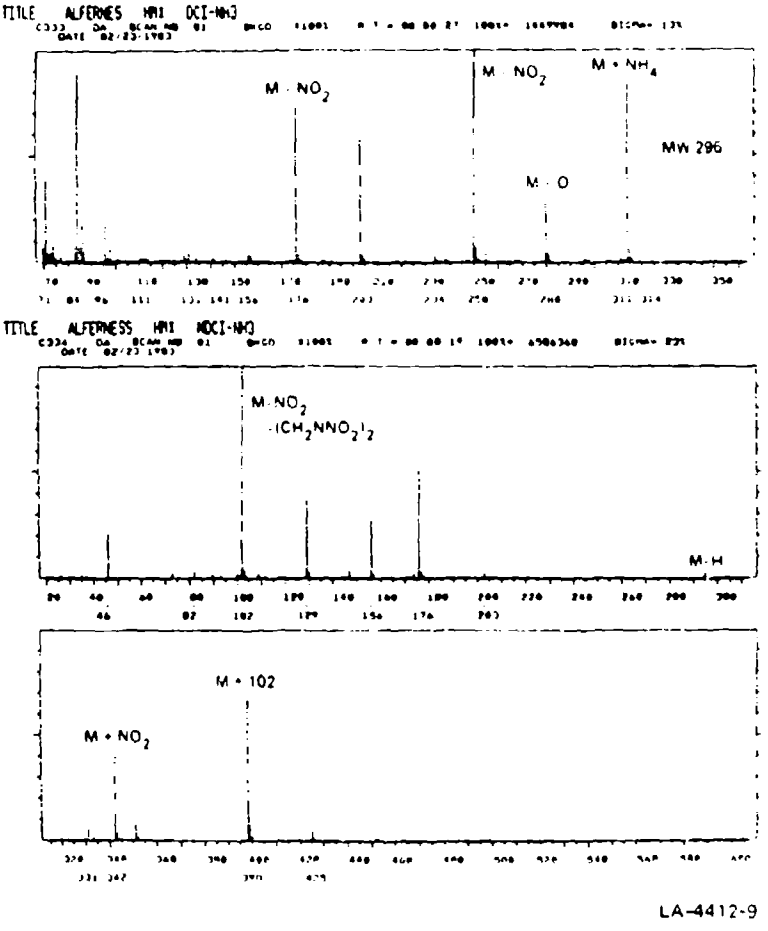

FIGURE 9 MASS SPECTRA FOR HMX

(a) Positive ion (b) Negative ion

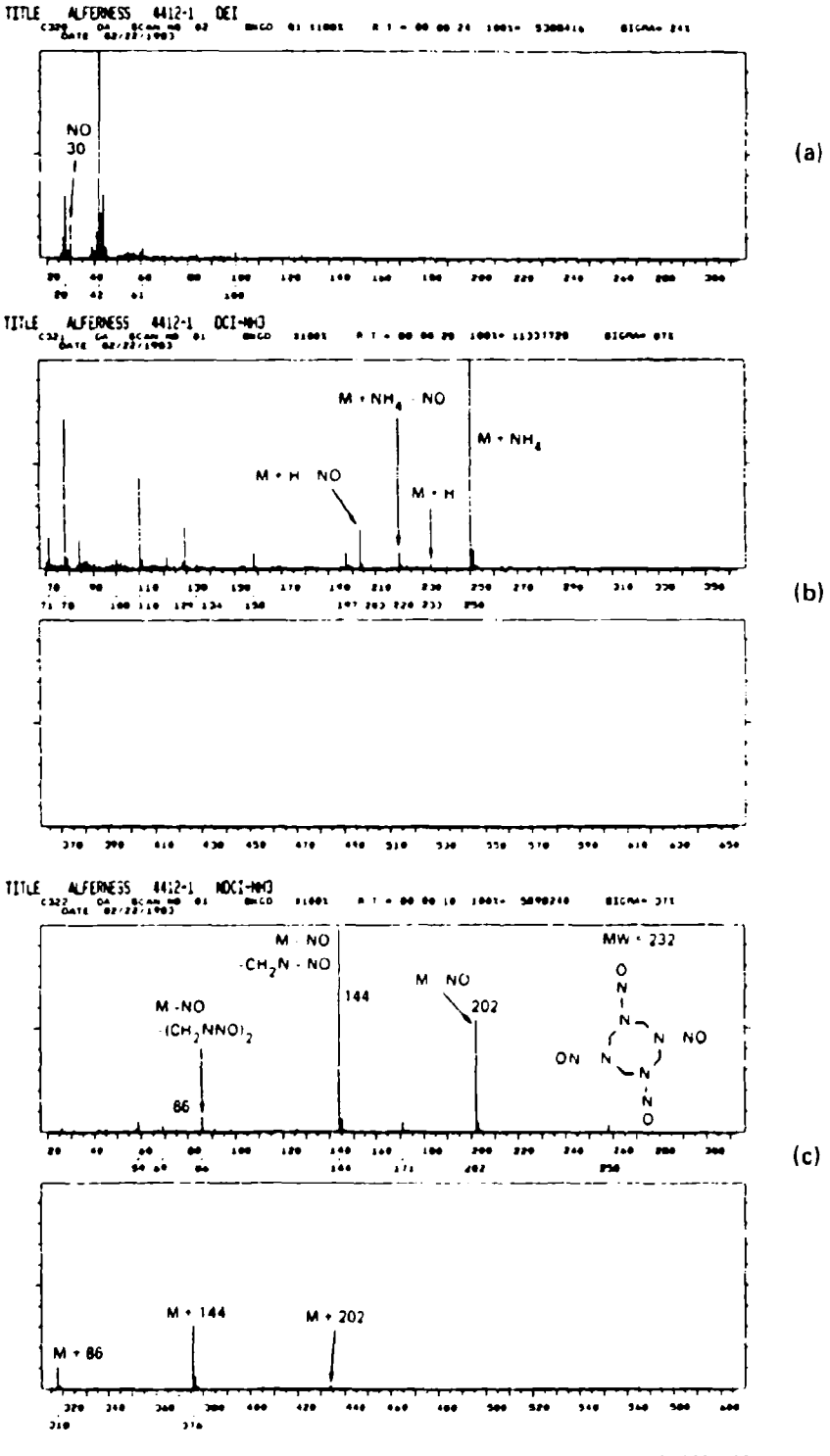

FIGURE 10 MASS SPECTRA FOR METABOLITE I

(a) Electron impact (b) Positive ion (c) Negative ion

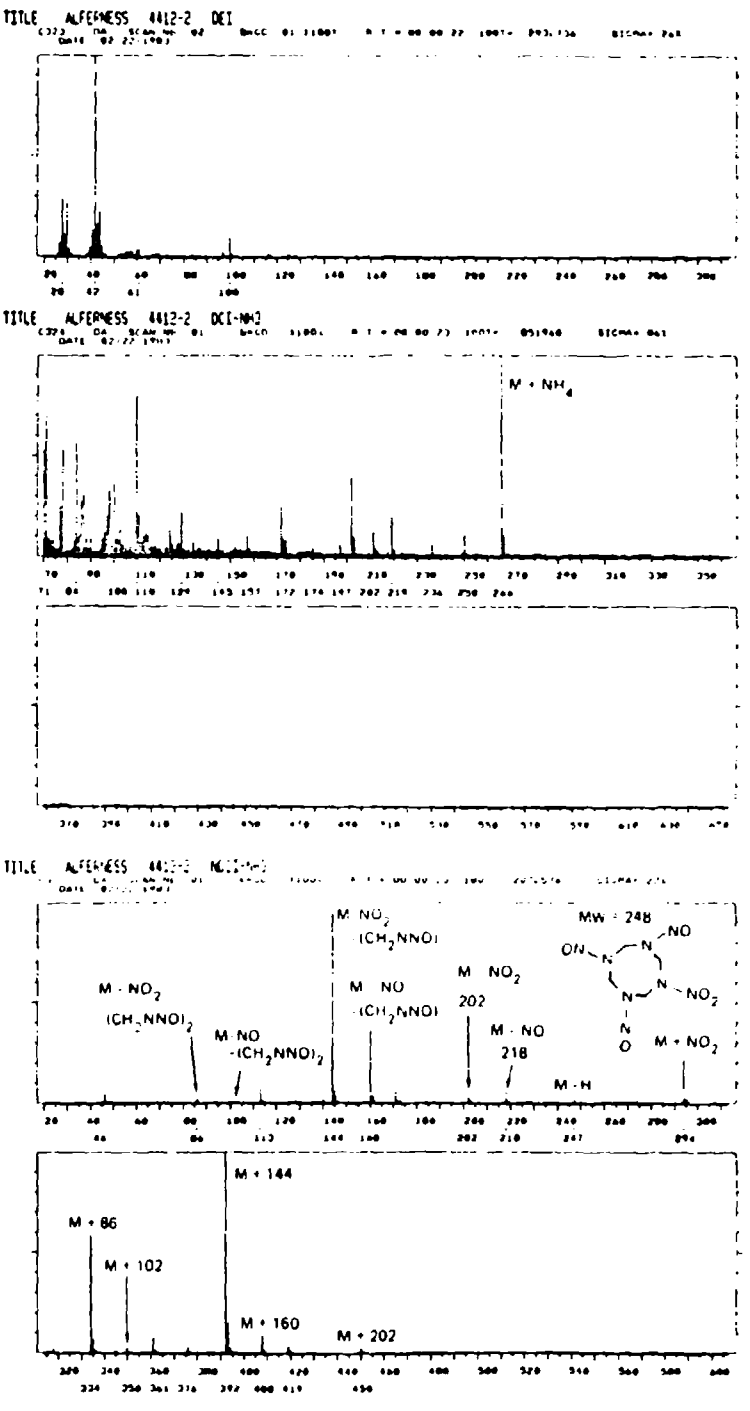

FIGURE 11 MASS SPECTRA FOR HMX METABOLITE II

(a) Electron impact (b) Positive ion (c) Negative ion

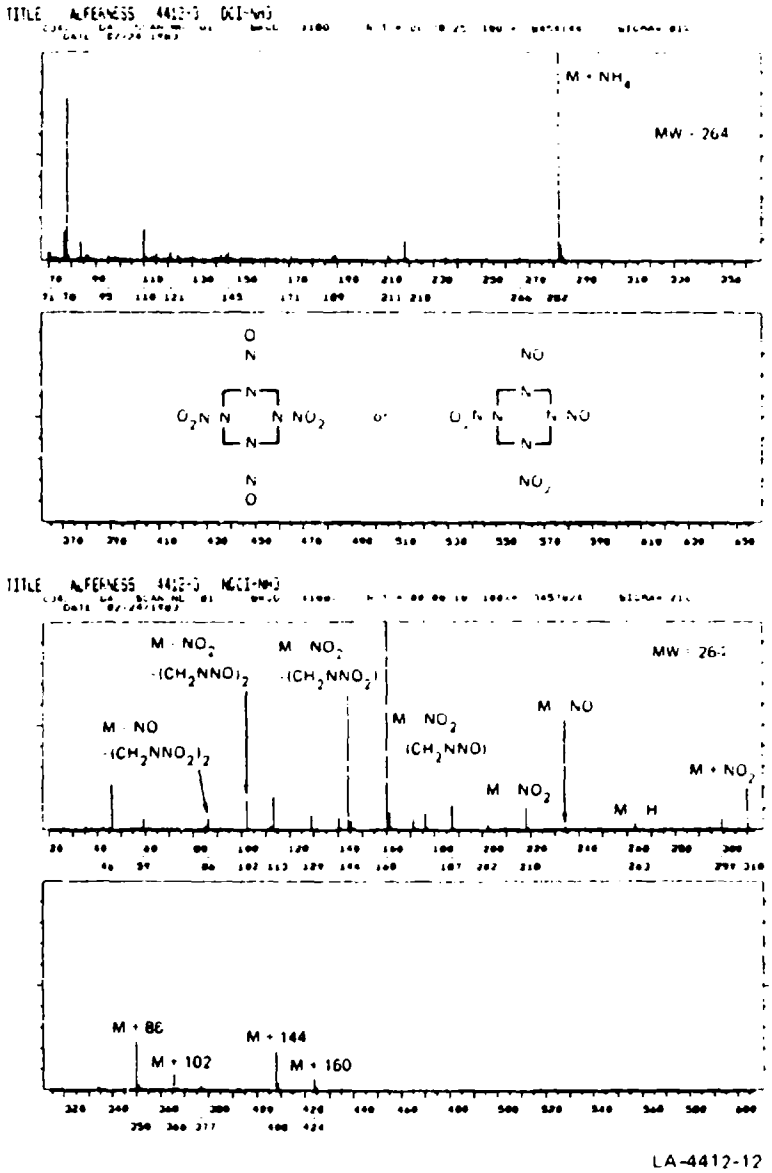

FIGURE 12 MASS SPECTRA FOR HMX METABOLITE III

(a) Positive ion (b) Negative ion

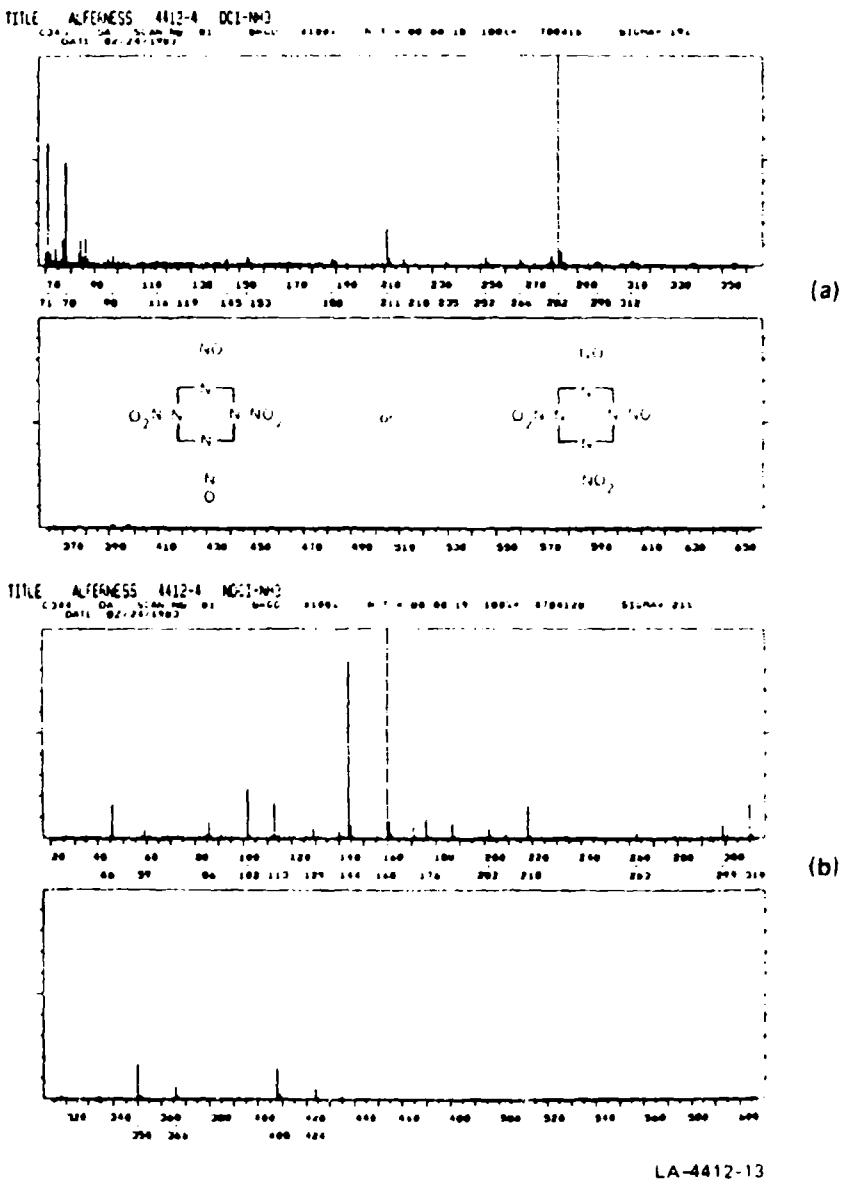

FIGURE 13 MASS SPECTRA FOR HMX METABOLITE IV

(a) Positive ion (b) Negative ion

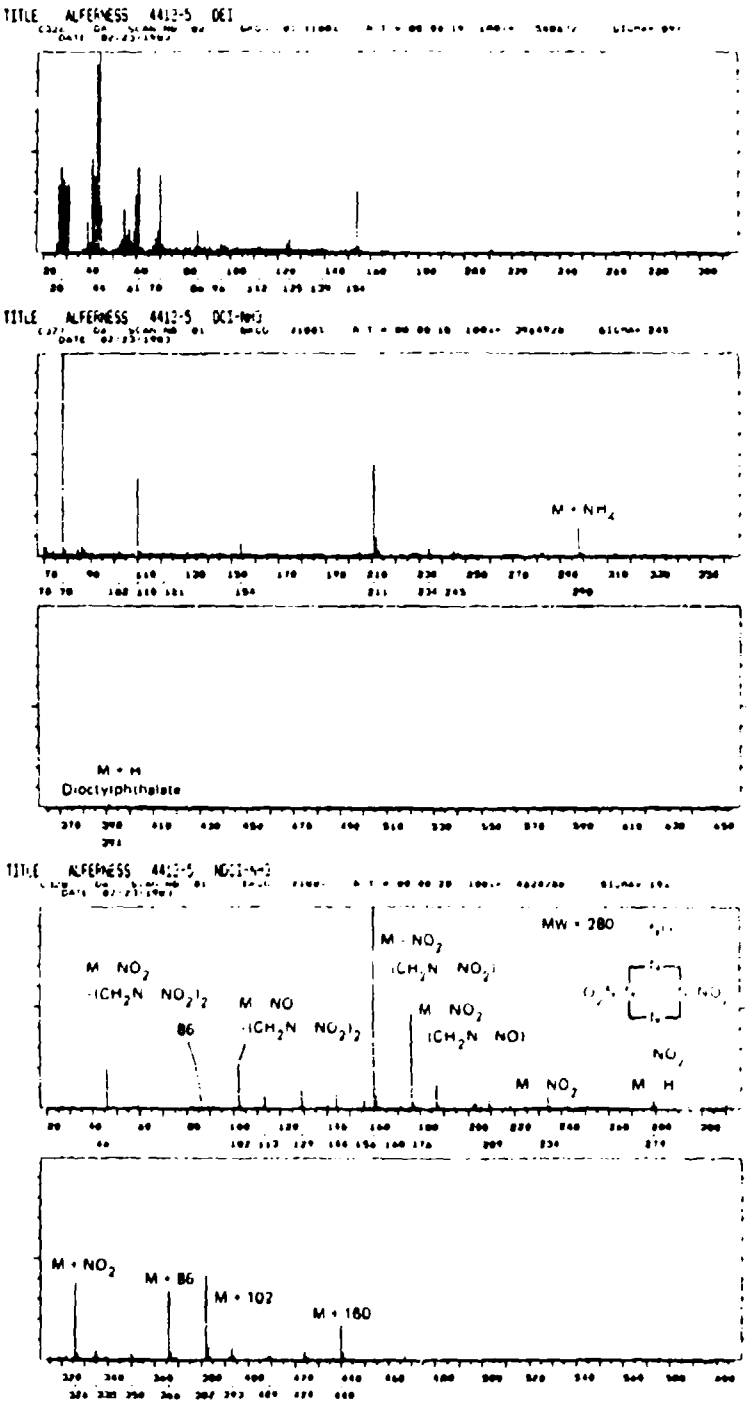

FIGURE 14 MASS SPECTRA FOR HMX METABOLITE V
(a) Electron impact (b) Positive ion (c) Negative ion

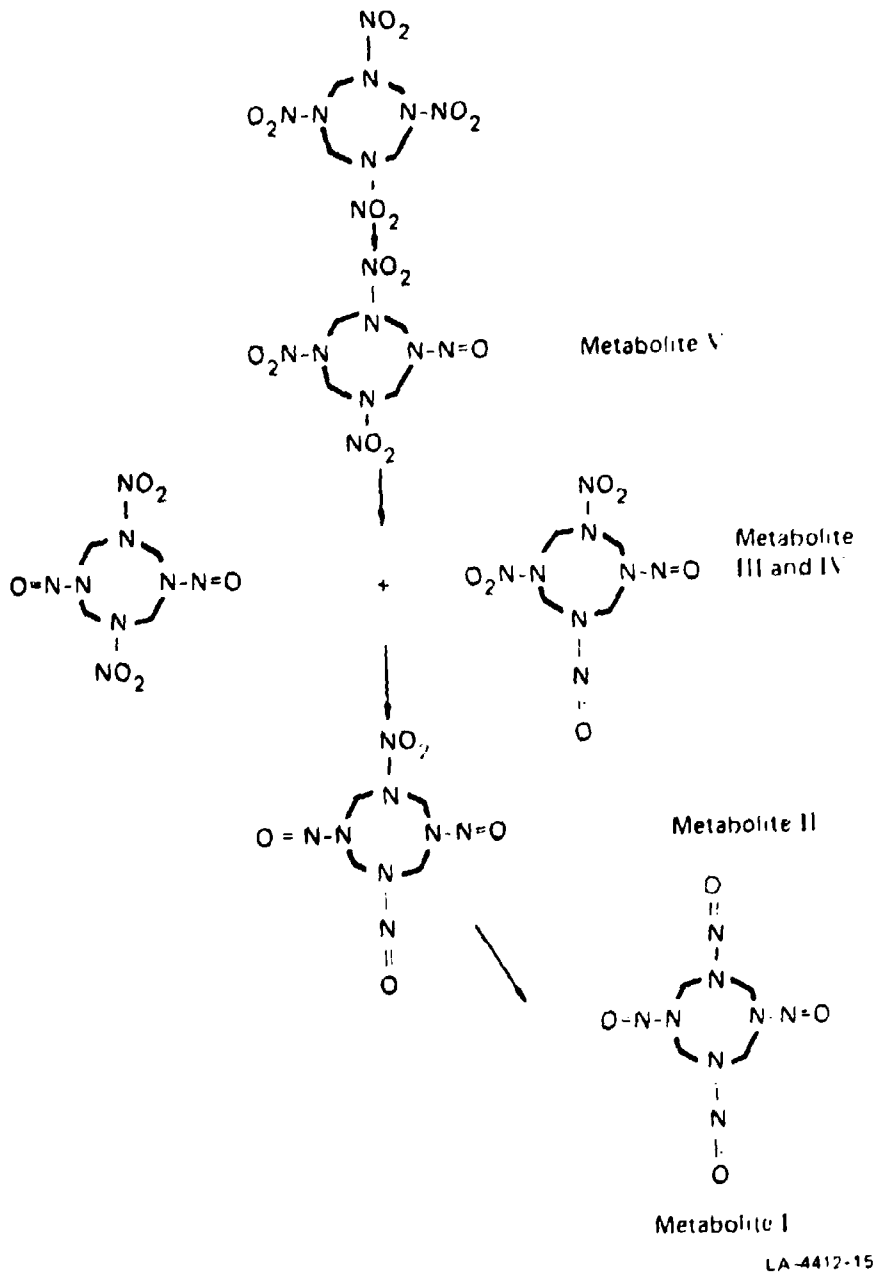

FIGURE 15 ANAEROBIC METABOLISM OF HMX

These reductive metabolites also appeared in the sample of aerobic biotransformation waters. The microorganisms may obtain electrons from metabolism of organic nutrients which may be used for the nitro reduction.

The organisms are capable of further reductive transformation of the nitroso derivatives. In our experiment, a 100-ml aliquot of biotransformation solution was adjusted to pH 10 and distilled. The distillate was acidified and rotary-evaporated to dryness. Acetic anhydride was added to the residue, which was heated for 10 min at 70°C, and analyzed by gas chromatography/mass spectrometry. 1,1-Dimethylhydrazine was identified as an HMX transformation product and confirmed with an authentic standard. Thus, successive reductions of HMX in nutrient-rich environments can significantly transform HMX.

4. Biotransformation Discussion

From our results, it appears that HMX can be biotransformed aerobically or anaerobically in freshly collected wasteline water and in the presence of small amounts of organic nutrients such as 50 ppm of yeast extract. The water sample collected from the wasteline pipe or the Holston River all supported aerobic biotransformation, except for the wasteline water collected on June 7. When the remaining waste waters were stored under refrigeration, the biotransformation capability diminished. The filamentous fungus in the wasteline water was not considered to be responsible for the HMX biotransformation because it did not transform HMX under the conditions for its abundant growth.

Yeast extract alone or mixed with acetate, propionate, and benzoate provided nutrient for the transformation of HMX in fresh water, but these nutrients could not maintain the transformation organisms. Possibly other nutrients or physical conditions are necessary for the enrichment of this culture. Nevertheless, aerobic HMX-biotransforming bacteria are present in the Holston wastestream and may transform part of the HMX in the wastewater. Some nutrients in the wastewater or

certain environmental conditions are necessary to maintain these organisms. However, in the Holston River, the levels of organisms and nutrients may be too low for biotransformation to play a significant role.

The anaerobic biotransformation of HMX was as expected due to its structural simularity to RDX and our previous studies (Spanggord et al, 1983) that showed rapid anaerobic biotransformation of RDX. The HMX degradation rate was also fairly fast using 50 ppm of yeast extract or other organic nutrients. The organic nutrient appeared to be needed for the biotransformation process as well as for bacterial growth. Therefore, anaerobic biotransformation appears to play an important role only in environments where anaerobic conditions exist and organic nutrients are present. The metabolic pathway was also similar to that of RDX degradation, as reported by McCormick et al. (1981) when successive reduction of the nitro groups to N-nitroso derivatives was reported followed by further metabolism.

D. Model Simulation

1. Holston River

In a previous study (Spanggord et al., 1981), we developed a two-dimensional river simulation model that simulated the flow of the Holston River at the point where wastestreams emanating from HAAP entered the Holston River to a location (Surgoinsville) 20 km from the discharge point. The model was applied to assess the loss and movement of HMX in the Holston River.

Briefly, HAAP wastestreams entering the Holston River, flowing at 90 to 121 $m^3\ s^{-1}$, do not become uniformly mixed for at least 20 km from the discharge point. Therefore, HMX migrates in a lateral direction (north bank to south bank) as well as in the direction of flow. We compartmentalized the Holston River, as shown in Figure 16, to account for lateral flow and investigated the loss and movement of HMX along the north bank, center, and south bank of the Holston River.

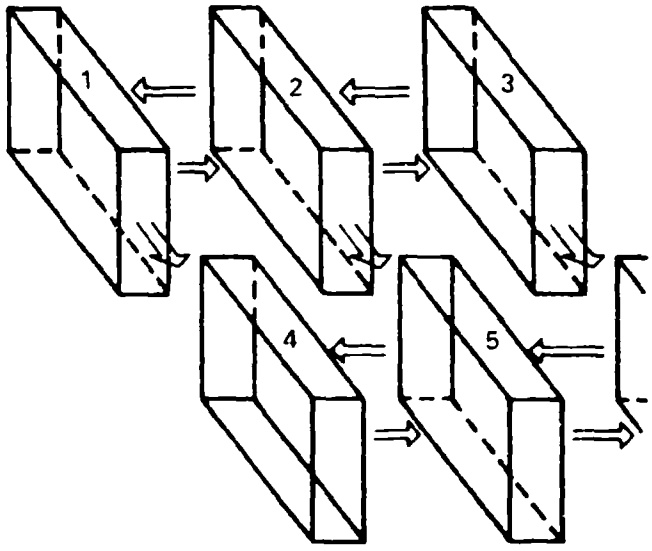

FIGURE 16 PHYSICAL CONFIGURATION OF A TWO-DIMENSIONAL RIVER SIMULATION

For these investigations, only photolysis was considered as the dominant process leading to transformation, because the nutrient dependence and low bacterial population did not favor biotransformation. Using an initial HMX input concentration of 0.46 ppm (wastestream concentration; Spanggord et al., 1981) and a photolysis rate constant of 6.3 d^{-1} cm for the summer months, HMX concentrations were simulated for the north, center, and south portions of the Holston River for 20 km. The results are shown in Figure 17. The primary factor contributing to changes in HMX concentration over the first 20 km is dilution, with photolysis contributing to approximately a 5% loss in the summer months. Transformation losses of only 1% are predicted for the winter months. These two examples represent the extreme cases for potential transformation of HMX in the Holston River. The photolysis transformation process can be accelerated by shallow low-flow river conditions or slowed by deep, high-flow river conditions. Under normal river flow conditions, we expect that HMX will persist for a significant distance from HAAP, with dilution serving as the primary mechanism of HMX concentration reduction.

2. LAAP Lagoon

The Louisiana Army Ammunition Plant disposal lagoons have been described (Spanggord et al., 1983). Lagoon No. 9 is a flat-bottomed, rectangular basin measuring 56.7 m × 52.1 m. It is filled with a dark amber-colored water to a depth of approximately 60 m in the winter; the depth fluctuates throughout the year according to rainfall and evaporation rates. The color of the water is derived from the photolysis products of 2,4,6-trinitrotoluene (TNT) and attenuates the ability of light to penetrate significantly into the water. Measured photolysis rate constants for HMX were found to be 20 times greater in pure water compared with lagoon water (Table 3). However, using a computer simulation model developed for TNT, we simulated the loss of HMX from lagoon No. 9 using photolysis rate constants ranging from 0.0048 cm d^{-1} in winter to 0.0288 cm d^{-1} in summer and an initial

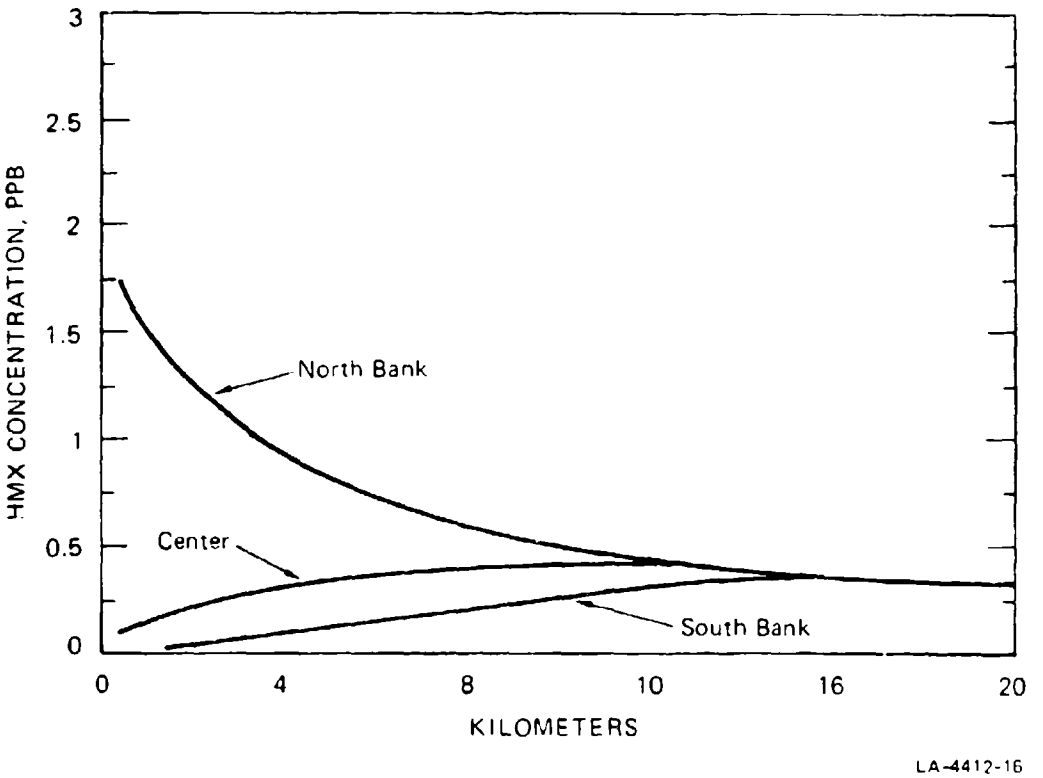

FIGURE 17 SIMULATED HMX CONCENTRATIONS IN THE NORTH, CENTER, AND SOUTH PORTIONS OF THE HOLSTON RIVER AS A FUNCTION OF DISTANCE FROM THE HMX DISCHARGE STREAM

imput concentration of 2.0 ppm. The simulation results are shown in Figure 18. The results show that HMX is persistent in the lagoon over the simulation period (8 months). The concentration of HMX gradually rises due to water evaporation in the summer months until its solubility limit is reached (12 ppm at 41°C) in late August. Superimposed on the simulation graph are actual data points measured by Spanggord et al. (1983), which show a gradual increase in lagoon HMX concentration as a function of time of year. These data correlate reasonably well with the simulation results.

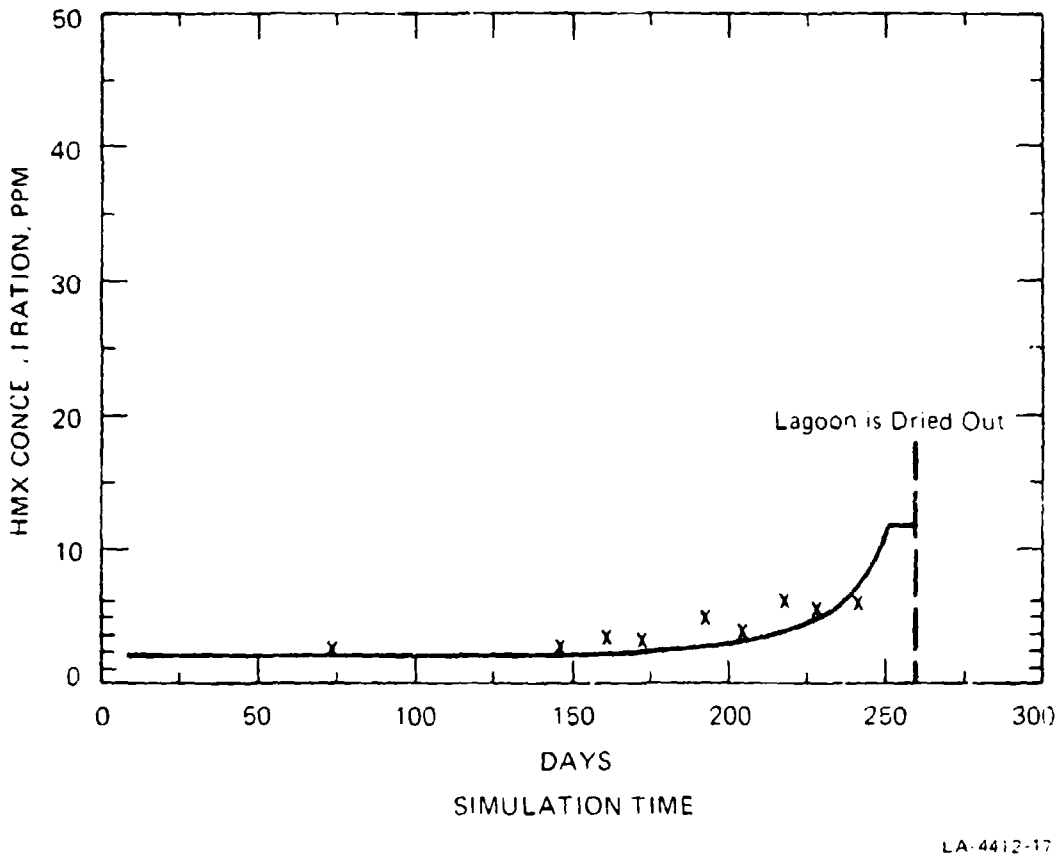

FIGURE 18 SIMULATION OF HMX CONCENTRATION IN LAAP LAGOON AS A FUNCTION OF DAY OF YEAR

IV. DISCUSSION

The results of this study suggest that photolysis will be the primary transformation pathway for HMX loss in the environment, with an average half-life of 17 days in the Holston River (150 cm deep) and 7900 days in LAAP laggon water. The transformation products appear to be innocuous or readily assimilated by aquatic organisms. Photolysis proceeds by a direct photolytic mechanism in which light is absorbed and transformation occurs with an efficiency of 13%. Factors that slow the transformation process are those that attenuate light entering the water body, such as high water absorptivity, as observed in the LAAP lagoon, or depth, as observed in the Holston River. Coupled to these factors are seasonal variations in light intensity, which can be as large as a factor of 5 between summer and winter months. Thus, a worst-case condition for HAAP would be a high HMX discharge concentration during the winter months under high river-flow conditions. Similarly, the greatest extent of transformation would occur in summer months when the river is shallow and moving slowly. A similar set of conditions could be proposed for the LAAP lagoon, except that as the lagoon becomes shallow (through evaporation), the photic zone becomes smaller due to concentration of the light-absorbing species. Thus, although transformation rates are projected to be faster in the summer months, a linear relationship with light intensity is not expected.

The aerobic and anaerobic biotransformation studies showed that HMX can be transformed under special conditions of freshly collected water and supplemental organic nutrients, but in no case was the transformation observed in wastewater or Holston River water alone. Also, no enriched culture that utilize HMX as a sole carbon and energy source could be isolated. Based on these data, no biotransformation rate constant was projected for the Holston River.

In the presence of supplemental organic nutrients (yeast extract), the transformation proceeded quite readily, with a half-life of 17 hr under aerobic conditions (bacterial population of 2×10^7 CFU ml^{-1}) and 2 hr under anaerobic conditions (bacterial population of 3×10^7 CFU ml^{-1}). Under both conditions, the transformation involved the reduction of a nitro group leading to mono- to tetra nitroso derivatives of HMX. Further reduction of the nitroso group leads to derivatives such as 1,1-dimethylhydrazine, which was identified in the incubated solutions. We were able to detect trace amounts of the mono-, di-, and tetranitroso biotransformation products of HMX in the HAAP HMX wastestream by comparative retention times; however, confirmation of the identification could not be made. No metabolites were observed in the Holston River. We might expect that conditions favoring biotransformation may occur in the Holston River through upstream pollutant discharge or sewage disposal. These conditions represent isolated events and are not representative of normal conditions in the Holston River. Thus, although biotransformation would be a significant transformation process, favorable conditions for this transformation were not evident in the Holston River.

No studies were performed on the biotransformation of HMX in LAAP lagoon waters. We assumed that biotransformation would not be significant based on studies performed by Spanggord et al. (1983), which showed RDX biotransformation to be insignificant in the lagoon environment. This was projected by the model simulation and verified by actual lagoon sampling data (Spanggord et al., 1983).

The computer model simulation projected that HMX concentrations would persist for significant distances past HAAP. If an HMX discharge of 450 ppb is reduced to 0.3 ppb at Surgoinsville (20 km from discharge site), we would expect to find 0.2 ppb at Knoxville (125 km from the discharge site) in the summer months, assuming that further dilutions would be minimal. We might expect Morristown (70 km from discharge point) residents who use Holston River water as a water supply to intake approximately 0.25 ppb HMX in their water. This

example represents the type of projection of chemical concentration that can be made by model simulation at distant points based on chemical input, river flow, and seasonal variation and demonstrates the applicability of fate data to overall hazard assessments.

In conclusion, the results of this study indicate that HMX will be persistent in the studied environments, with dilution serving as the major factor in reducing HMX concentration. In the case of HAAP, controlling the HMX concentration in the wastestream should result in HMX concentrations in the Holston River that are acceptable to mammalian and aquatic populations. In the case of lagoon disposals of HMX, HMX concentrations are expected to increase in water bodies where the light attenuation is high (resulting from TNT photolysis). Lagoon disposal of HMX waste (and RDX) could be a viable treatment procedure in UV light-transmissive water bodies.

V. REFERENCES

Cotton, F.A., and G. Wilkinson (1967). Advanced Inorganic Chemistry. Interscience Publishers, New York.

Glover, D.J., and J.C. Hoffsommer (1979). Photolysis of RDX. Identification and Reactions of Products. Report NS SWCTR 79-349, Naval Surface Weapons Center, Silver Spring, MD.

Lamberton, A.H., C. Lindley, and J.C. Speakman (1979). Studies on nitroamines. Part VII. The decomposition of methylenedinitroamine in Aqueous Solution. J. Chem. Soc. Vol 1650-1656.

McCormick, N.G., J.H. Cornell, and A.M. Kaplan (1981). Biodegradation of hexahydro-1,3,5-trinitro-1,3,5-triazine. Appl. Environ. Microbiol. 42, 817-823.

Smith, J.H., W.R. Mabey, N. Bohonos, B.R. Holt, S.S. Lee, T.W. Chou, D.C. Bomberger, and T. Mill (1978). Environmental Pathways of Selected Chemicals in Freshwater Systems. Part II, Laboratory Studies. Final Report, EPA Contract 68-03-2227, SRI International, Menlo Park, CA.

Spanggord, R.J., W.R. Mabey, T.W. Chou, D.L. Haynes, P.L. Alferness, D.S. Tse, and T. Mill (1982). Environmental Fate Studies of HMX, Phase I, Screening Studies. Final Report, USAMRDC Contract DAMD17-82-C-2100, SRI International, Menlo Park, CA.

Spanggord, R.J., W.R. Mabey, T. Mill, T.W. Chou, J.H. Smith, and S. Lee (1981). Environmental Fate Studies on Certain Munition Wastewater Constitutents, Phase III, Part 1, Model Validation. Final Report, USAMRDC Contract DAMD17-78-C-8081, SRI International, Menlo Park, CA.

Spanggord, R.J., W.R. Mabey, T. Mill, T.W. Chou, J.H. Smith, S. Lee, and D. Roberts (1983). Environmental Fate Studies on Certain Munition Wastewater Constituents, Phase IV, Lagoon Model Studies. Final Report, USAMRDC Contract DAMD17-78-C-8081, SRI International, Menlo Park, CA.

Thayer, J.R. (1979). Rapid Simultaneous Determination of Nitrate and Nitrate. Altex Chromatogram 3, 2-3.

Zafirou, O.C. (1974). Sources and reactions of OH and daughter radicals in seawater. J. Geophys. Res. 79, 4491-4497.

Zepp, R.G., and D.M. Cline (1977). Rates of Direct Photolysis in Aquatic Environments. Environ. Sci. Technol. 11, 359-366.

DISTRIBUTION LIST

25 copies	Commander US Army Medical Bioengineering Research and Development Laboratory ATTN: SGRD-UBG Fort Detrick, Frederick, MD 21701
4 copies	Commander US Army Medical Research and Development Command ATTN: SGRD-RMS Fort Detrick, Frederick, MD 21701
12 copies	Defense Technical Information Center (DTIC) ATTN: DTIC-DDA Cameron Station Alexandria, VA 22314
1 copy	Dean School of Medicine Uniformed Services University of the Health Sciences 4301 Jones Bridge Road Bethesda, MD 20014
1 copy	Commandant Academy of Health Sciences, US Army ATTN: AHS-CDM Fort Sam Houston, TX 78234
1 copy	Commander US Army Medical Bioengineering Research and Development Laboratory ATTN: SGRD-UBD-A/Librarian Fort Detrick, Frederick, MD 21701